

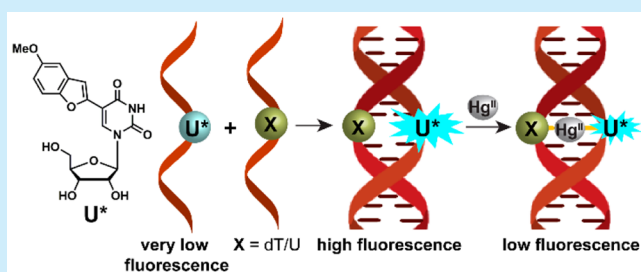
Synthesis and Enzymatic Incorporation of a Responsive Ribonucleoside Probe That Enables Quantitative Detection of Metallo-Base Pairs

Sudeshna Manna and Seergazhi G. Srivatsan*¹

Department of Chemistry, Indian Institute of Science Education and Research (IISER) Pune, Dr. Homi Bhabha Road, Pune 411008, India

Supporting Information

ABSTRACT: Synthesis of a highly responsive fluorescent ribonucleoside analogue based on a 5-methoxybenzofuran uracil core, enzymatic incorporation of its triphosphate substrate into RNA transcripts, and its utility in the specific detection and estimation of Hg²⁺-ion-mediated metallo-base pair formation in DNA–RNA and RNA–RNA duplexes are described.



Selective binding of metal ions to natural and modified nucleobases has rendered such noncanonical metallo-base pairs as useful motifs to devise tools to sense and trap heavy-metal ions, detect single-nucleotide polymorphism, and fabricate electronic wires and nanomachines.^{1,2} In particular, pyrimidine-metal-pyrimidine base pairs formed by Hg²⁺ and Ag⁺ ions have received significant attention, because of their diagnostic and material applications³ and recent findings linking the metal toxicity and mutagenicity to metallo-base pair formation.^{3a,4} It is now clear that T-Hg²⁺-T can serve as a stable analogue of T-A pair⁵ and could potentially introduce mutations by facilitating enzymatic misincorporation of dTTP opposite to T.⁶ A recent study demonstrates that the addition of Hg²⁺ ions to duplexes containing T-T mismatch significantly reduces the efficiency of DNA polymerase activity, compared to equivalent duplexes containing T-A pair, suggesting that the metallo-base pair can hamper the DNA metabolism.⁴ Similarly, in the presence of Ag⁺ ions, the DNA polymerases do incorporate dATP/dTTP/dCTP opposite to dC, which is largely dependent on the sequence and substrate/enzyme concentration.⁷

Several biophysical methods, including ultraviolet (UV), nuclear magnetic resonance (NMR), electron paramagnetic resonance (EPR), X-ray, and isothermal titration calorimetry (ITC) methods are commonly used to study metallo-base pair structure, kinetics, and thermodynamics.⁸ Alternatively, fluorescence resonance energy transfer (FRET)-pair-labeled T-rich oligonucleotides (ONs), hairpin-forming motifs, and a thrombin binding aptamer have been developed to monitor the formation and stability of metallo-base pairs.⁹ Similarly, label-free Hg²⁺ and Ag⁺ sensors have been developed by using intercalating organic dyes and metal complexes, which show changes in fluorescence upon metal ion-induced base pairing.¹⁰ Usually, these methods use higher concentrations of ON

duplexes and or stretches of T-T mismatches to obtain reliable response upon base-pair formation.^{1b,3} However, detecting and estimating site-specific nucleobase-metal interactions in duplexes at submicromolar concentrations would provide a better understanding of their actual biological impact (e.g., point mutations and conformation changes induced by metal ion binding).⁴ In this context, environment-sensitive fluorescent nucleoside analogues based on a dimethylaminobenzene core and pyrrolo-dC were successfully used in detecting and determining the local kinetics and thermodynamic parameters of metallo-base pairs formed by Hg²⁺ and Ag⁺ ions in DNA ON duplexes.¹¹ However, to the best of our knowledge, there is no report that describes the fluorescence analysis of site-specific metallo-base pair interaction in DNA–RNA heteroduplexes and RNA–RNA duplexes. Such an effort, apart from aiding material design, could also be useful in understanding the impact of metallo-base pairs in RNA folding, function, and recognition.

Here, we report the development of a new microenvironment-sensitive ribonucleoside analogue, 5-methoxybenzofuran uridine (1), which after triphosphorylation (2) serves as a good substrate for RNA polymerase in *in vitro* transcription reaction and selectively reports dT-1 and U-1 mismatches in model DNA–RNA and RNA–RNA ON duplexes, respectively, with significant enhancement in fluorescence. This property of the nucleoside analogue was aptly utilized in establishing a method to selectively detect single Hg²⁺-mediated base pair in different duplexes. Furthermore, by monitoring the changes in fluorescence intensity as a function

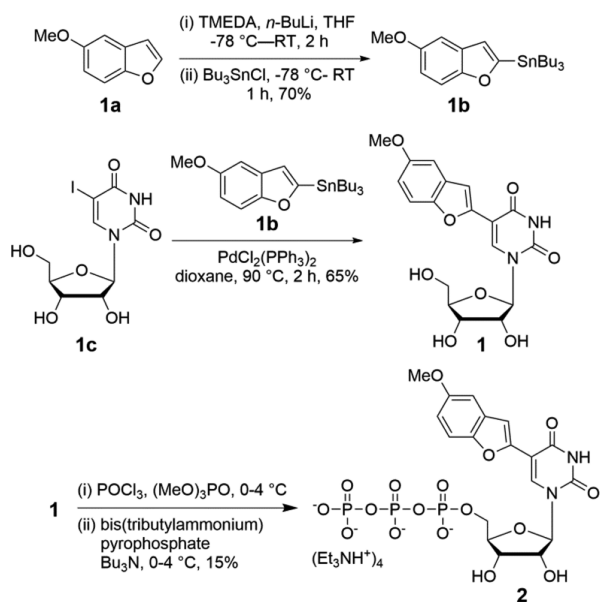
Received: May 2, 2019

Published: June 7, 2019

of Hg^{2+} ion concentration, it was found that the metal ion binds to dT–U better than the U–U mismatch.

It has been shown that conjugating or fusing heterocyclic rings onto purine and pyrimidine bases can produce responsive nucleoside analogues.¹² Their implementation in nucleic acid analysis has been largely empirical, based on the fluorescence outcome in model systems. Following a similar probe design approach, 5-methoxybenzofuran uridine **1** was synthesized according to the steps given in Scheme 1. 5-Methoxybenzofur-

Scheme 1. Synthesis of Nucleoside 1 and Its Triphosphate 2



an (**1a**) was first stannylated and then cross-coupled with 5-iodouridine (**1c**) in the presence of a palladium catalyst under Stille reaction conditions. The corresponding triphosphate substrate **2** required for *in vitro* transcription was synthesized by reacting nucleoside **1** with POCl_3 , followed by a reaction with pyrophosphate (Scheme 1).

Photophysical analysis in solvents of different polarity and viscosity confirmed the environment-sensitive nature of the nucleoside analogue. The longest wavelength absorption maximum of **1** was found to be slightly red-shifted and hyperchromic as the polarity was reduced from water to methanol to dioxane (see Figure 1 and Table 1). Notably, the nucleoside exhibited excellent fluorescence solvatochromism (Figure 1, Table 1). In water, it was practically nonemissive, and, with a change in solvent polarity, the quantum yield increased dramatically by 250-fold in the least polar solvent tested (dioxane). The emission maximum was also found to be significantly blue-shifted. Interestingly, a comparison of relative quantum yields ($\Phi_x/\Phi_{\text{water}}$) of **1** and few other heterocycle-conjugated nucleoside probes¹³ in different solvents, as a function of $E_T(30)$ (Reichardt's microscopic solvent polarity parameter) revealed that nucleoside **1** is highly sensitive to even small changes in micropolarity (Figure S1 in the Supporting Information). Other probes showed very small differences in the quantum yield. As the solvent viscosity was increased from water to ethylene glycol to glycerol, the quantum yield also increased significantly, because of rigidification of the fluorophore, which was further confirmed by the higher anisotropy values exhibited by the probe in a more-viscous medium (see Figure 1 and Table 1).¹⁴ While the viscosity of

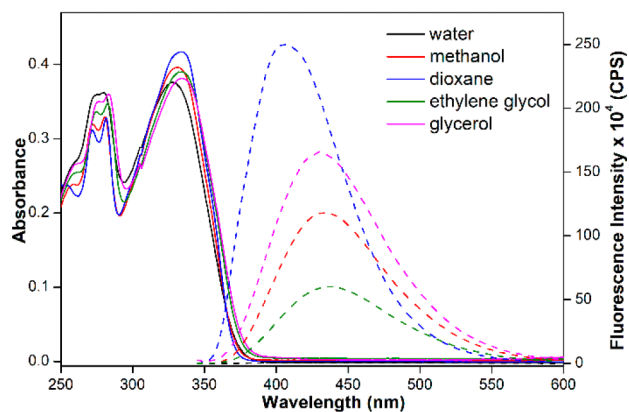


Figure 1. Absorption ($25 \mu\text{M}$, solid lines) and emission ($5.0 \mu\text{M}$, dashed lines) spectra of nucleoside **1** in different solvents. See the Supporting Information (SI) for details.

Table 1. Fluorescence Properties of Nucleoside Analogue 1

solvent	λ_{max}^a (nm)	λ_{em}^a (nm)	$E_T(30)$	Φ^b	$\Phi_x/\Phi_{\text{water}}^c$	r^d
water	329	–	63.1	0.0008	1	nd
methanol	331	433	55.5	0.11	137	nd
dioxane	335	406	36.0	0.20	250	0.03
ethylene glycol	332	435	56.3	0.07	88	0.26
glycerol	335	430	57.2	0.21	263	0.33

^aThe lowest energy absorption maximum is given. ^bThe standard deviation of Φ in water is 0.00006, and in other solvents, it is ≤ 0.004 . ^cRelative quantum yield ($\Phi_x/\Phi_{\text{water}}$), where x is the solvent. ^dThe standard deviation of r (anisotropy) in different solvents is ≤ 0.004 ; nd = not determined.

methanol and dioxane is considerably lower, compared to that of ethylene glycol and glycerol, higher or comparable fluorescence efficiency suggests that the fluorescence outcome in different solvents is largely due to a polarity effect.

To evaluate the responsiveness in duplexes, we sought to incorporate nucleoside analogue **1** into RNA transcripts by *in vitro* transcription reaction, using modified nucleoside 5'-triphosphate **2**. The templates were custom-made to contain one or two dA residues in the coding region to guide the incorporation of modified nucleoside **1** into the transcripts (Figure 2). To facilitate easy visualization of full-length transcription products by phosphor imaging, all templates contained a dT at the 5' end to guide the incorporation of an $\alpha\text{-}^{32}\text{P}$ adenosine label. Transcription was initiated by adding T7 RNA polymerase to a reaction mixture containing T7 promoter-template duplex, GTP, CTP, UTP/2, and $\alpha\text{-}^{32}\text{P}$ ATP, and was resolved by PAGE under denaturing conditions (see Figure 3, as well as Figure S2 in the SI). Using template T1, singly modified full-length transcript **4** was formed in very good yields (81%, Figure 3, lane 2). Incorporation of nucleoside **1** was evident from the slower mobility exhibited by transcript **4**, compared to native transcript **3**. Along with the full-length product, trace amounts of nontemplated incorporation products were also formed, which is common in *in vitro* transcription reactions. Importantly, when UTP or **2** was not added, full-length product was not formed, which indicated that there was no random misincorporation of the nucleotide analogue (Figure 3, lane 3). Notably, when the reaction was performed in the presence of an equimolar concentration of **2** and UTP, both of the triphosphates were incorporated with

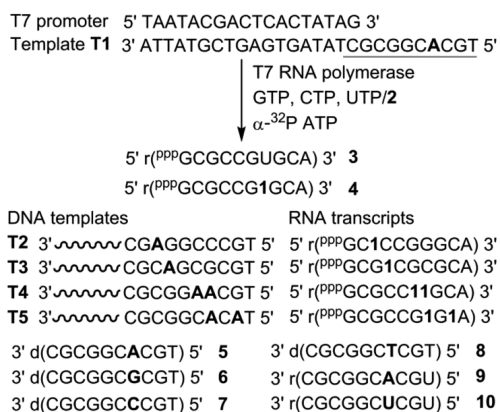


Figure 2. Enzymatic incorporation of triphosphate 2 into RNA ON transcripts in the presence of DNA templates T1–T5. Complementary and mismatched ONs (3–10) used in this study. Prefixes “d” and “r” represent DNA and RNA ONs, respectively.

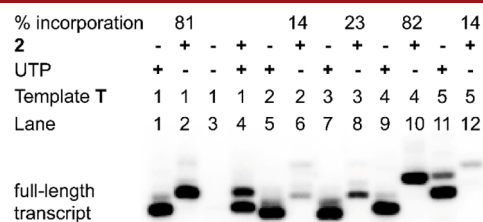


Figure 3. Phosphor image of PAGE resolved transcription products obtained using DNA templates T1–T5 in the presence of UTP and or 2. See Figure S2 in the SI for a complete gel picture and conditions.

comparable efficiency (Figure 3, lane 4). Reactions with other templates indicated that modifications near the promoter region using T2 and T3 were less tolerated and adjacently placed modification using T4 was produced in good yields, compared to nucleoside analogue placed in an alternating position using T5 (Figure 3, lanes 5–12). Furthermore, modified transcript 4 obtained from a large-scale reaction with T1 was purified and its purity and integrity were confirmed by HPLC, mass analysis, and enzymatic digestion (see Figures S3 and S4 and Table S1 in the SI).

To understand the behavior of nucleoside 1 in different neighboring base environment, a model RNA transcript 4 labeled with 1 was hybridized to complementary DNA and RNA ONs (Figure 2). The duplexes were designed such that the emissive base was placed opposite to complementary and mismatched bases. The emissive analogue placed opposite to a complementary base dA/A (4•5 and 4•9) and mismatched bases dG and dC (4•6 and 4•7) showed comparable fluorescence intensity (Figure 4). Notably, when placed opposite to dT (4•8) or U (4•10), nucleoside 1 showed a significant enhancement in fluorescence intensity, compared to other duplexes (see Figure 4, as well as Figure S5 in the SI). Thus, the emissive analogue 1 was able to selectively detect dT and U mismatches in a DNA–RNA and RNA–RNA hetero and homo duplexes, respectively. CD analysis suggests that hybrid duplexes and RNA duplexes adopt a similar secondary structure, which resembles the A-form (Figure S6 in the SI). In the absence of further structural information, it is proposed that small differences in stacking interaction and electron transfer between the fluorophore and adjacent bases, the solvation–desolvation effect, and rigidification–derigidification

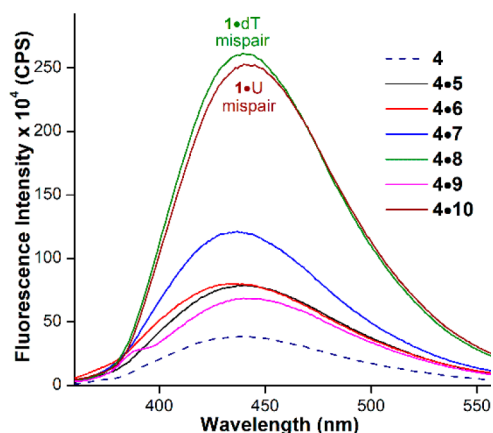


Figure 4. Emission spectra of duplexes (1 μ M) formed by hybridizing transcript 4 with complementary and mismatched DNA and RNA ONs (5–10).

of the fluorophore could have influenced the fluorescence outcome.^{14,15}

The ability of the probe to signal dT and U mismatches was put to use in devising a simple fluorescence method to detect and estimate metallo base-pairs as we envisioned that Hg²⁺ ion binding to these mismatches could alter the electronics, as well as the environment of the probe, thus, influencing its fluorescence.^{11,16} Rewardingly, the addition of 1 equiv of Hg²⁺ ions significantly reduced the fluorescence intensity of duplexes 4•8 and 4•10 containing dT and U mismatches, respectively (see Figure 5, as well as Figure S7 in the SI).

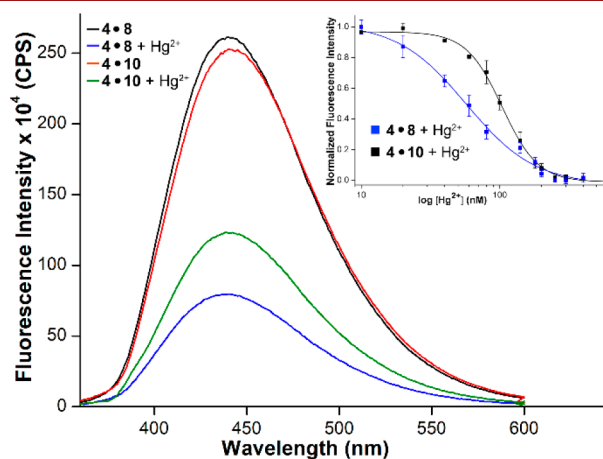


Figure 5. Fluorescence spectra of duplexes 4•8 and 4•10 (1 μ M) in the presence and absence of Hg²⁺ ions (1 μ M). Inset shows the curve fit for the titration of duplexes with Hg²⁺ ions. See the SI for details.

However, free nucleoside 1, single-stranded RNA ON 4, and perfect and other mismatched duplexes displayed only minor differences in fluorescence in the presence and absence of Hg²⁺ ions (see Figure S7). Furthermore, as compared to Hg²⁺ ions, the addition of 1 equiv of different metal ions (Ag⁺, Ca²⁺, Cu²⁺, Cd²⁺, Pb²⁺, Mn²⁺, Mg²⁺, Co²⁺, Zn²⁺, Fe²⁺, and Ni²⁺) had only a minor influence on the fluorescence of duplexes containing the probe placed opposite to dT and U mismatches (see Figure S8 in the SI). These findings confirm that our probe reliably and selectively reports Hg²⁺ ion-mediated metallo-base pair formation in DNA–RNA and RNA–RNA duplexes. The reduction in fluorescence intensity in the presence of Hg²⁺ is

more likely due to the base-paired state of the nucleoside analogue, which experiences more stacking interaction and quenching effect from adjacent guanosine bases.^{11b,15,16} Furthermore, the fluorescence could also be quenched by the coordinated heavy atom.⁴

The responsiveness of the probe also enabled determination of the binding affinity of the Hg²⁺ ion to duplexes. Titrating with the metal ion resulted in a dose-dependent quenching in fluorescence intensity, which gave an apparent dissociation constant K_d of 57 ± 7 nM for **4•8** and 104 ± 2 nM for **4•10** (see Figure 5, as well as Figure S9 in the SI). While K_d values are in the range observed for the dT–Hg²⁺–dT pair, our results suggest that the metal ion has a comparatively higher binding affinity for dT–U mismatch in a DNA–RNA duplex than U–U mismatch in an RNA–RNA duplex.

The formation of dT–Hg–1 and U–Hg–1 base pairs was ascertained by performing the following experiments. In the presence of Hg²⁺ ions, both control (**3•8**, **3•10**) and modified duplexes (**4•8**, **4•10**) showed significant increase in thermal melting ($\Delta T_m = 17$ – 21 °C) due to stabilization of the mispairs by metal ion coordination (see Figure S10 and Table S2 in the SI). As expected, perfect duplexes (**3•5**, **4•5**, **3•9**, and **4•9**) showed only minor differences in T_m upon the addition of Hg²⁺ ions (see Table S2). Furthermore, the addition of increasing concentrations of the metal ion to duplexes **4•8** and **4•10** resulted in the complete disappearance of respective imino proton signals (10.6 and 10.4 ppm, corresponding to mispair) at 1 equiv of the Hg²⁺ ion (see Figure S11 in the SI). Consistent with the literature reports,^{11a} these results confirm that the label is minimally perturbing and the fluorescence response is a true reflection of the formation of metallo base-pairs.

In summary, we have introduced a new fluorescent ribonucleoside analogue that is minimally perturbing, highly sensitive to its local environment, and a good substrate for T7 RNA polymerase. The analogue incorporated into an RNA transcript and hybridized to complementary and mismatched ONs served as a fluorescence turn-on reporter for dT and U mismatches. This behavior was used in the specific detection and estimation of Hg²⁺-mediated metallo-base pair formation. It was found that the Hg²⁺ ion binds relatively better to a dT mispair in a hybrid duplex, compared to a U mispair in a RNA homo duplex. Taken together, the utility of our probe and these findings are important, because it could further elucidate the implications of metallo-base pairs in RNA folding and recognition.

■ ASSOCIATED CONTENT

Supporting Information

The Supporting Information is available free of charge on the ACS Publications website at DOI: 10.1021/acs.orglett.9b01544.

Experimental details, characterization data, supporting figures and tables (PDF)

■ AUTHOR INFORMATION

Corresponding Author

*E-mail: srivatsan@iiserpune.ac.in

ORCID

Seergazhi G. Srivatsan: 0000-0001-5765-3967

Notes

The authors declare no competing financial interest.

■ ACKNOWLEDGMENTS

S.M. thanks UGC, India for a graduate research fellowship. This work was supported by Wellcome Trust-DBT India Alliance (No. IA/S/16/1/S02360) grant to S.G.S.

■ REFERENCES

- (1) (a) Clever, G. H.; Kaul, C.; Carell, T. DNA–Metal base pairs. *Angew. Chem., Int. Ed.* **2007**, *46*, 6226–6236. (b) Tanaka, Y.; Kondo, J.; Sychrovský, V.; Šebera, J.; Dairaku, T.; Saneyoshi, H.; Urata, H.; Torigoe, H.; Ono, A. Structures, physicochemical properties, and applications of T–Hg^{II}–T, C–Ag^I–C, and other metallo-base-pairs. *Chem. Commun.* **2015**, *51*, 17343–17360. (c) Zhou, W.; Saran, R.; Liu, J. Metal sensing by DNA. *Chem. Rev.* **2017**, *117*, 8272–8325.
- (2) (a) Ono, A.; Togashi, H. Highly selective oligonucleotide-based sensor for mercury(II) in aqueous solutions. *Angew. Chem., Int. Ed.* **2004**, *43*, 4300–4302. (b) Hollenstein, M.; Hipolito, C.; Lam, C.; Dietrich, D.; Perrin, D. M. A highly selective DNzyme sensor for mercuric ions. *Angew. Chem., Int. Ed.* **2008**, *47*, 4346–4350. (c) Dave, N.; Chan, M. Y.; Huang, P.-J. J.; Smith, B. D.; Liu, J. Regenerable DNA-functionalized hydrogels for ultrasensitive, instrument-free mercury(II) detection and removal in water. *J. Am. Chem. Soc.* **2010**, *132*, 12668–12673. (d) Lin, Y.-W.; Ho, H.-T.; Huang, C.-C.; Chang, H.-T. Fluorescence detection of single nucleotide polymorphisms using a universal molecular beacon. *Nucleic Acids Res.* **2008**, *36*, No. e123. (e) Wang, Z.-G.; Elbaz, J.; Remacle, F.; Levine, R. D.; Willner, I. All-DNA finite-state automata with finite memory. *Proc. Natl. Acad. Sci. U. S. A.* **2010**, *107*, 21996–22001. (f) Liu, S.; Clever, G. H.; Takezawa, Y.; Kaneko, M.; Tanaka, K.; Guo, X.; Shionoya, M. Direct conductance measurement of individual metallo-DNA duplexes within single-molecule break junctions. *Angew. Chem.* **2011**, *123*, 9048–9052. (g) Tanaka, K.; Clever, G. H.; Takezawa, Y.; Yamada, Y.; Kaul, C.; Shionoya, M.; Carell, T. Programmable self-assembly of metal ions inside artificial DNA duplexes. *Nat. Nanotechnol.* **2006**, *1*, 190–194. (h) Kim, E.-K.; Switzer, C. Bis(6-carboxypurine)-Cu²⁺: a possibly primitive metal-mediated nucleobase pair. *Org. Lett.* **2014**, *16*, 4059–4061.
- (3) (a) Ono, A.; Torigoe, H.; Tanaka, Y.; Okamoto, I. Binding of metal ions by pyrimidine base pairs in DNA duplexes. *Chem. Soc. Rev.* **2011**, *40*, 5855–5866. (b) Scharf, P.; Müller, J. Nucleic acids with metal-mediated base pairs and their applications. *ChemPlusChem* **2013**, *78*, 20–34.
- (4) Schmidt, O. P.; Mata, G.; Luedtke, N. W. Fluorescent base analogue reveals T–Hg^{II}–T base pairs have high kinetic stabilities that perturb DNA metabolism. *J. Am. Chem. Soc.* **2016**, *138*, 14733–14739.
- (5) Miyake, Y.; Togashi, H.; Tashiro, M.; Yamaguchi, H.; Oda, S.; Kudo, M.; Tanaka, Y.; Kondo, Y.; Sawa, R.; Fujimoto, T.; Machinami, T.; Ono, A. Mercury^{II}-mediated formation of thymine–Hg^{II}–thymine base pairs in DNA duplexes. *J. Am. Chem. Soc.* **2006**, *128*, 2172–2173.
- (6) (a) Urata, H.; Yamaguchi, E.; Funai, T.; Matsumura, Y.; Wada, S.-I. Incorporation of thymine nucleotides by DNA polymerases through T–Hg^{II}–T base pairing. *Angew. Chem., Int. Ed.* **2010**, *49*, 6516–6519. (b) Funai, T.; Nakamura, J.; Miyazaki, Y.; Kiriu, R.; Nakagawa, O.; Wada, S.-i.; Ono, A.; Urata, H. Regulated incorporation of two different metal ions into programmed sites in a duplex by DNA polymerase catalyzed primer extension. *Angew. Chem., Int. Ed.* **2014**, *53*, 6624–6627. (c) Park, K. S.; Jung, C.; Park, H. G. "Illusionary" polymerase activity triggered by metal ions: use for molecular logic-gate operations. *Angew. Chem., Int. Ed.* **2010**, *49*, 9757–9760.
- (7) Funai, T.; Miyazaki, Y.; Aotani, M.; Yamaguchi, E.; Nakagawa, O.; Wada, S.; Torigoe, H.; Ono, A.; Urata, H. Ag^I ion mediated formation of a C–A mispair by DNA polymerase. *Angew. Chem., Int. Ed.* **2012**, *51*, 6464–6466.

- (8) (a) Tanaka, Y.; Oda, S.; Yamaguchi, H.; Kondo, Y.; Kojima, C.; Ono, A. ^{15}N – ^{15}N J-Coupling Across Hg^{II} : Direct observation of Hg^{II} -Mediated T–T Base Pairs in a DNA duplex. *J. Am. Chem. Soc.* **2007**, *129*, 244–245. (b) Yamaguchi, H.; Šebera, J.; Kondo, J.; Oda, S.; Komuro, T.; Kawamura, T.; Dairaku, T.; Kondo, Y.; Okamoto, I.; Ono, A.; Burda, J. V.; Kojima, C.; Sychrovský, V.; Tanaka, Y. The structure of metallo-DNA with consecutive thymine– Hg^{II} –thymine base pairs explains positive entropy for the metallo base pair formation. *Nucleic Acids Res.* **2014**, *42*, 4094–4099. (c) Torigoe, H.; Miyakawa, Y.; Ono, A.; Kozasa, T. Positive cooperativity of the specific binding between Hg^{2+} ion and T:T mismatched base pairs in duplex DNA. *Thermochim. Acta* **2012**, *532*, 28–35. (d) Jakobsen, U.; Shelke, S. A.; Vogel, S.; Sigurdsson, S. T. Site-directed spin-labeling of nucleic acids by click chemistry: detection of abasic sites in duplex DNA by EPR spectroscopy. *J. Am. Chem. Soc.* **2010**, *132*, 10424–10428. (e) Liu, H.; Cai, C.; Haruehanroengra, P.; Yao, Q.; Chen, Y.; Yang, C.; Luo, Q.; Wu, B.; Li, J.; Ma, J.; Sheng, J.; Gan, J. Flexibility and stabilization of Hg^{II} -mediated C:T and T:T base pairs in DNA duplex. *Nucleic Acids Res.* **2016**, *45*, 2910–2918.
- (9) (a) Wang, Z.; Lee, J. H.; Lu, Y. Highly sensitive “turn-on” fluorescent sensor for Hg^{2+} in aqueous solution based on structure-switching DNA. *Chem. Commun.* **2008**, 6005–6007. (b) Teh, H. B.; Wu, H.; Zuo, X.; Li, S. F. Y. *Sensors and Actuators B*. Detection of Hg^{2+} using molecular beacon-based fluorescent sensor with high sensitivity and tunable dynamic range. *Sens. Actuators, B* **2014**, *195*, 623–629. (c) Liu, C.-W.; Huang, C.-C.; Chang, H.-T. Chang, H.-T. Highly selective DNA-based sensor for lead(II) and mercury(II) ions. *Anal. Chem.* **2009**, *81*, 2383–2387.
- (10) (a) Chan, D. S.-H.; Lee, H.-M.; Che, C.-M.; Leung, C.-H.; Ma, D.-L. A selective oligonucleotide-based luminescent switch-on probe for the detection of nanomolar mercury(II) ion in aqueous solution. *Chem. Commun.* **2009**, 7479–7481. (b) Zhang, X.; Li, Y.; Su, H.; Zhang, S. Highly sensitive and selective detection of Hg^{2+} using mismatched DNA and a molecular light switch complex in aqueous solution. *Biosens. Bioelectron.* **2010**, *25*, 1338–1343. (c) Wang, Y.; Geng, F.; Xu, H.; Qu, P.; Zhou, X.; Xu, M. A label-free oligonucleotide based thioflavin-T fluorescent switch for Ag^+ detection with low background emission. *J. Fluoresc.* **2012**, *22*, 925–929. (d) Ma, D.-L.; He, H.-Z.; Leung, K.-H.; Zhong, H.-J.; Chan, D. S.-H.; Leung, C.-H. Label-free luminescent oligonucleotide-based probes. *Chem. Soc. Rev.* **2013**, *42*, 3427–3440.
- (11) (a) Schmidt, O. P.; Benz, A. S.; Mata, G.; Luedtke, N. W. Hg^{II} binds to C–T mismatches with high affinity. *Nucleic Acids Res.* **2018**, *46*, 6470–6479. (b) Park, K. S.; Lee, J. Y.; Park, H. G. Mismatched pyrrolo-dC-modified duplex DNA as a novel probe for sensitive detection of silver ions. *Chem. Commun.* **2012**, *48*, 4549–4551.
- (12) (a) Sinkeldam, R. W.; Greco, N. J.; Tor, Y. Fluorescent analogs of biomolecular building blocks: design, properties, and applications. *Chem. Rev.* **2010**, *110*, 2579–2619. (b) Tanpure, A. A.; Pawar, M. G.; Srivatsan, S. G. Fluorescent nucleoside analogs: probes for investigating nucleic acid structure and function. *Isr. J. Chem.* **2013**, *53*, 366–378.
- (13) (a) Pawar, M. G.; Nuthanakanti, A.; Srivatsan, S. G. Heavy atom containing fluorescent ribonucleoside analog probe for the fluorescence detection of RNA-ligand binding. *Bioconjugate Chem.* **2013**, *24*, 1367–1377. (b) Pawar, M. G.; Srivatsan, S. G. Synthesis, photophysical characterization, and enzymatic incorporation of a microenvironment-sensitive fluorescent uridine analog. *Org. Lett.* **2011**, *13*, 1114–1117. (c) Tanpure, A. A.; Srivatsan, S. G. A Microenvironment-sensitive fluorescent pyrimidine ribonucleoside analogue: synthesis, enzymatic incorporation, and fluorescence detection of a DNA abasic site. *Chem. - Eur. J.* **2011**, *17*, 12820–12827. (d) Milisavljević, N.; Perlíková, P.; Pohl, R.; Hocek, M. Enzymatic synthesis of base-modified RNA by T7 RNA polymerase. A systematic study and comparison of 5-substituted pyrimidine and 7-substituted 7-deazapurine nucleoside triphosphates as substrates. *Org. Biomol. Chem.* **2018**, *16*, 5800–5807.
- (14) (a) Sinkeldam, R. W.; Wheat, A. J.; Boyaci, H.; Tor, Y. Emissive nucleosides as molecular rotors. *ChemPhysChem* **2011**, *12*, 567–570.
- (b) Dziuba, D.; Jurkiewicz, P.; Cebecauer, M.; Hof, M.; Hocek, M. A Rotational BODIPY nucleotide: an environment-sensitive fluorescence-lifetime probe for DNA interactions and applications in live-cell microscopy. *Angew. Chem., Int. Ed.* **2016**, *55*, 174–178. (c) Manna, S.; Sarkar, D.; Srivatsan, S. G. A dual-app nucleoside probe provides structural insights into the human telomeric overhang in live cells. *J. Am. Chem. Soc.* **2018**, *140*, 12622–12633.
- (15) (a) Rachofsky, E. L.; Osman, R.; Ross, J. B. A. Probing structure and dynamics of DNA with 2-aminopurine: effects of local environment on fluorescence. *Biochemistry* **2001**, *40*, 946–956. (b) Doose, S.; Neuweiler, H.; Sauer, M. Fluorescence quenching by photoinduced electron transfer: a reporter for conformational dynamics of macromolecules. *ChemPhysChem* **2009**, *10*, 1389–1398. (c) Teppang, K. L.; Lee, R. W.; Burns, D. D.; Turner, M. B.; Lokensgard, M. E.; Cooksy, A. L.; Purse, B. W. Electronic Modifications of fluorescent cytidine analogues control photophysics and fluorescent responses to base stacking and pairing. *Chem. - Eur. J.* **2019**, *25*, 1249–1259.
- (16) (a) Kim, S. J.; Kool, E. T. Sensing metal ions with DNA building blocks: fluorescent pyridobenzimidazole nucleosides. *J. Am. Chem. Soc.* **2006**, *128*, 6164–6171. (b) Blanchard, D. J. M.; Manderville, R. A. An internal charge transfer-DNA platform for fluorescence sensing of divalent metal ions. *Chem. Commun.* **2016**, *52*, 9586–9588.